Journal of Power Sources 192 (2009) 423–428

Contents lists available at ScienceDirect

Journal of Power Sources

journal homepage: www.elsevier.com/locate/jpowsour

New anodic diffusive layer for passive micro-direct methanol fuel cell

Ting Yuan[a,b], Zhiqing Zou[a], Mei Chen[a,b], Zhilin Li[a], Baojia Xia[a], Hui Yang[a,*]

[a] Energy Science and Technology Laboratory, Shanghai Institute of Microsystem and Information Technology, Chinese Academy of Sciences, Shanghai 200050, China
[b] Graduate School of the Chinese Academy of Sciences, Beijing 100039, China

ARTICLE INFO

Article history:
Received 10 February 2009
Received in revised form 19 March 2009
Accepted 19 March 2009
Available online 27 March 2009

Keywords:
Anodic diffusive layer
Passive micro-DMFC
Membrane electrode assembly
Carbon nanotubes
Electrochemical impedance

ABSTRACT

The addition of carbon nanotubes (CNTs) into anodic micro-porous layer (MPL) of the membrane electrode assembly significantly improves the performance of the passive micro-direct methanol fuel cells (DMFCs). The maximum power density of ca. 32.2 mW cm^{-2} at a temperature of ca. 25 °C and under air-breathing mode is achieved with pure CNTs as anode MPL material. Impedance analysis and cyclic voltammetric measurements of the anodes indicate that the increased performance of the passive DMFC with the addition of CNTs into anodic MPLs could be attributed to the decrease in charge transfer resistance of the anode reaction and to the improvement in catalyst utilization. Scanning electron microscopy measurements show the network formation within the MPL due to the one-dimensional structure of CNTs, which could be beneficial to the methanol mass transfer and to the improvement in catalyst utilization. Furthermore, the durability test of a passive DMFC after 300 h operation demonstrates that the passive DMFC with CNTs as anode MPL materials exhibits very good stability.

1. Introduction

The direct methanol fuel cell (DMFC) is regarded as a potential power source for portable applications due to its high energy density, simplicity, easy fuel-recharging and low pollution [1–3]. However, there are several technological issues that have to be addressed before its practical applications. These challenges include the crossover of methanol from the anode to the cathode, sluggish kinetics of both anode and cathode reactions, the management of water and heat, relatively low power density and limited lifetime [4].

The passive DMFC is an attractive candidate for portable power application because of its simplicity. For a passive DMFC system, fuel and oxidant are supplied to the electrodes only depending on diffusion, thus additional devices or components such as electronic fans, compressors and peristalsis pumps may not be necessary, which would decrease the volume of such a system, reduce substantial weight and parasitic power, and decrease the cost of the full fuel cell system [5]. Therefore, the effective mass transfer of both fuel and oxidant becomes an important factor for the performance improvement of a passive DMFC. Under the passive DMFC operation, the anode pores must allow methanol to reach the catalyst active sites and support the gas pathways for the removal of CO_2 bubble, and the cathode pores must support the gas pathways to O_2 or air and provide an efficient transport of water at the same time [6].

During the last decade, much attention has been paid to the improvement in efficient oxygen mass transfer on cathode side of the DMFCs. For example, Lin et al. [7] employed the heated-spraying technique for the preparation of the cathodic micro-porous layer (MPL); thus, resulting in a higher mass transfer rate of oxygen and a better performance of a DMFC than that with the conventional MPL. Chen and Zhao [8] found that the utilization of metal foam as the cathode diffusion layer could lead to an improvement in cell performance due to the enhanced transport of oxygen. More recently, Wang et al. [9] concluded that the addition of Ketjen Black EC 300J into the cathode catalyst layer increased the oxygen diffusion, Pt utilization and water removal capability. However, only few efforts have been made to improve the mass transfer efficiency of methanol on the anode side.

To improve the performance of a passive DMFC, methanol solution with high concentrations is commonly used to ensure the efficient mass transfer of methanol from the reservoir to the anode catalyst layer [10]. However, the use of high concentrated methanol solution will cause severe methanol crossover from the anode to the cathode, thus leading to a decrease in cell performance. Efforts to this end have involved (1) the modification of proton exchange membrane with palladium to reduce the methanol crossover [11,12]; (2) the development of new composite membranes [13]; and (3) the design of the membrane electrode assembly (MEA) with new structure, such as adding a hydrophilic thin film between the membrane and cathode catalyst layer to oxidize methanol permeated from the anode [14]. In the mean time, it has been recognized that the mass transport balance of methanol on anode side would play a crucial role in the improvement of methanol utilization with increased power density.

* Corresponding author. Tel.: +86 21 32200534; fax: +86 21 32200534.
E-mail addresses: hyang@mail.sim.ac.cn, huiyang65@hotmail.com (H. Yang).

0378-7753/$ – see front matter © 2009 Elsevier B.V. All rights reserved.
doi:10.1016/j.jpowsour.2009.03.032

Carbon nanotubes (CNTs) have been widely utilized as a catalyst support in fuel cells to enhance the catalytic activity due to their highly unusual structural, unique electrical properties, high surface area as well as a wide operational potential window [15–21]. For example, CNTs have been directly grown on carbon cloth and used as a support for Pt–Ru bimetallic catalysts for a DMFC [22,23]. Recently, Reshetenko et al. [5] optimized the structure and texture of the cathode by using CNTs as pore-forming additive, which leads to an increase in both the BET surface area and porosity of the electrode due to filamentous morphology of CNTs, thus improving the performance of an air-breathing DMFC. Wu et al. [24] reported that the addition of CNTs into anode catalytic layer of an MEA improved the performance of the DMFC, which was ascribed to the formation of continuous and uniform distribution of Nafion ionomer layer on the CNT surface to develop the pathways of proton transfer. However, the addition of CNTs into anodic MPL of a passive DMFC has not been reported for the performance improvement.

In this work, CNTs were used for the construction of anodic MPL to improve the performance of the passive DMFCs. It is believed that the addition of CNTs within the anodic MPL would lead to the formation of the network, thus improving the catalyst utilization and promoting the methanol mass transport through the MPL.

2. Experimental

2.1. MEA preparation

The membrane pretreatment procedures involved boiling the membrane in 5 vol.% H_2O_2 solution, washing with ultrapure water, boiling in 0.5 M H_2SO_4 solution and washing with ultrapure water for 2 h in turn. The pretreated membranes were kept in ultrapure water prior to the fabrication of MEAs.

A slurry which consisted of Vulcan XC-72 carbon and PTFE (20 wt.%) was coated onto the carbon paper (TGPH060, 20 wt.% PTFE, Toray) to form the cathodic MPL. The XC-72 carbon loading was ca. 2 mg cm^{-2}. For the preparation of anodic MPL, a slurry consisting of carbon materials and PTFE (20 wt.%) was coated onto the carbon paper (TGPH060, 0 wt.% PTFE, Toray) to form the anodic MPL. The total carbon loading was ca. 1 mg cm^{-2}. The carbon material used for anodic MPL was Vulcan XC-72, or CNTs (purified multi-walled carbon nanotubes), or a mixture of Vulcan XC-72 and CNTs with a mass ratio of 1:1. The CNTs used are commercial products from Shenzheng Nanotech. Port. Co. Ltd. without further functionalization.

The anode and cathode catalysts used in this work were Pt–Ru black with an atomic ratio 1:1 (HiSpec 6000, Johnson Matthey) and carbon-supported Pt with a Pt loading of 60 wt.% (HiSpec 9000, Johnson Matthey), respectively. Catalyst ink was prepared by dispersing appropriate amount of catalyst and 5 wt.% Nafion solution (Aldrich) into a mixture of isopropyl alcohol and ultrapure water with a volume ratio of 1:1. The catalyst ink was then sprayed on the MPL. The metal loading was 4.0 ± 0.2 mg cm^{-2} for both cathode and anode, and the ionomer loading was 20 wt.% for the cathode and 15 wt.% for the anode, respectively. The membrane electrode assembly was prepared by hot-pressing both anode and cathode on both sides of a pretreated Nafion117 membrane (H^+, DuPont) at 130 °C and 6 MPa for 3 min.

2.2. Single cell test

The MEA performance was evaluated in a single cell with an active cross-sectional area of 4 cm^2. The MEA was sandwiched between two Au-deposited stainless steel plates with open areas of ca. 33% for anode and cathode, respectively. Air was supplied to the electrodes only depending on diffusion through the open areas (air-breathing mode). A methanol solution reservoir was built in the anode fixture. Methanol was diffused into the catalyst layer from the built-in reservoir. There is no external pump used in our passive DMFC system. We have found that the better performance can be gained by using 2 M methanol solution as fuel in the passive DMFC system, similar to previous report [25].

The polarization curves of the passive DMFCs were obtained on an Arbin FCT testing system (Arbin Instrument Inc., USA). For each discharging current point along the polarization curve, a period of 2 min waiting time was used to obtain the stable voltage. The discharging curves at a constant voltage of 0.35 V were obtained for the passive DMFCs fueled with 6.0 mL of 2 M methanol solution. The test was not stopped until that the methanol in the reservoir was exhausted.

The durability of the MEAs with CNTs as anodic MPL material was tested in a single cell. The passive DMFC was discharged using an Arbin FCT testing system at a constant current density of 40 mA cm^{-2} for a period of time. During the discharging process, methanol solution was changed in about every 4 h.

2.3. Electrochemical characterizations

The electrochemical active surface area (ESA) of the anode catalyst layers was evaluated by cyclic voltammetry (CV) using an M273A Potentiostat/Galvanostat (EG&G, PAR) at a scan rate of 20 mV s^{-1}. During the test, the cathode was fed with humidified hydrogen, which served as the counter electrode and dynamic hydrogen electrode (DHE).

Electrochemical impedance spectra (EIS) were recoded using a Solartron SI2610 controlled by a personal computer and coupled to an M273A Potentiostat/Galvanostat. All anode impedance spectra recorded were measured between anode and DHE at the cathode, and the overpotential of the DHE is negligible according to the previous work [19]. Impedance spectra were obtained at a frequency range between 100 kHz and 0.01 Hz, and the amplitude of the sinusoidal voltage signal did not exceed 10 mV. The resulting impedance spectra were analyzed based on electrical circuit element model. The values of the model elements were determined by fitting the experimental data with Z-view software.

For all the electrochemical measurements, the cells were placed in a thermostated container at a temperature of ca. 25 ± 1 °C.

2.4. Surface morphology of the anodic MPLs

Surface morphology of the anodic MPLs was characterized by scanning electron microscopy (SEM) using a Hitachi S-4700 microscope operated at an accelerating voltage of 20.0 kV. SEM cross-sectional views of the MEA using pure CNTs as anodic MPL materials before and after long-term operation were characterized by using a JSM 6460 microscope operated at an accelerating voltage of 20.0 kV.

3. Results and discussion

3.1. Performance comparison of the passive DMFCs

Fig. 1 is a performance comparison of three passive micro-DMFCs by using different carbon materials within the anodic MPLs. It is clear that the open circuit voltage of the passive DMFC increases with the addition of CNTs into the anode MPLs. From the figure, the maximal power density of a passive DMFC with Vulcan XC-72 as anode MPL material is only 22.8 mW cm^{-2}, which is a comparative result with previously reported maximal power density of ca. 20 mW cm^{-2} for the passive DMFCs using Vulcan XC-72 as anodic MPL materials feeding with 2 M methanol solution [26,27]. When using a mixture of CNTs and Vulcan XC-72 with a mass ratio of

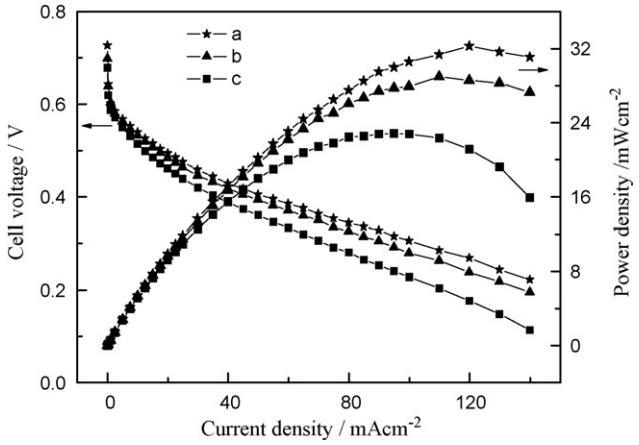

Fig. 1. Polarization curves of three passive DMFCs with (a) CNTs, (b) a mixture of CNTs and XC-72 carbon with a mass ratio of 1:1 and (c) XC-72 within the anodic MPLs using a 2 M methanol solution.

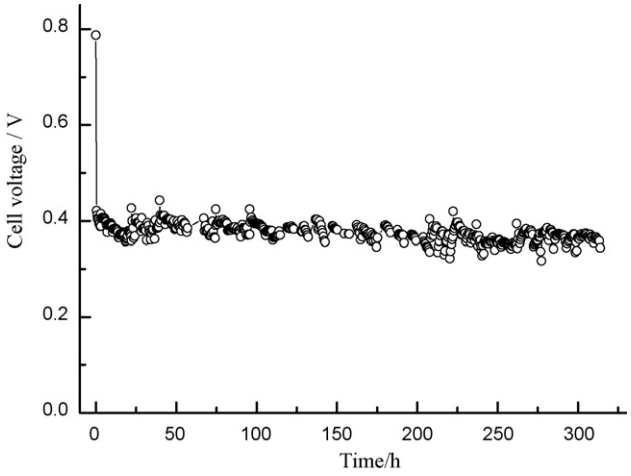

Fig. 3. Durability test of a single passive DMFC with CNTs as anodic MPL material at a discharging current density of 40 mA cm^{-2} using a 2 M methanol solution.

1:1, the maximal power density is about 28.9 mW cm^{-2}. However, the maximal power density of a passive DMFC by using pure CNTs within the anodic MPL exceeds 32.2 mW cm^{-2}; indicating that the addition of CNTs into the anodic MPL improves the power density of the passive DMFC. Such a power density of our passive DMFC with CNTs as anode MPL materials is comparative with previously results by Tsai et al. [22], in which a power density of 11.3 mW cm^{-2} mg^{-1} was obtained by using carbon nanotubes directly grown on carbon cloth as a gas diffusion layer. Moreover, the internal resistance of the DMFC decreases with the addition of CNTs into anode MPLs, suggesting that the addition of CNTs into the anodic MPL improves the contact between the MPL and catalytic layers. Furthermore, we have also found that the use of both single and double walled CNTs within the anodic MPLs would play a similar role in the performance improvement of the passive DMFCs to that of multiwalled CNTs, probably due to their one-dimensional structural characters.

To investigate the possible effects of CNTs on methanol mass transfer on anode side, two passive DMFCs with Vulcan XC-72 and CNTs as anode MPL materials were discharged at a constant voltage of 0.35 V, each cell fueled with 6.0 mL of 2 M methanol. Fig. 2 shows the discharging curves of two passive DMFCs. Clearly, the discharge current of the passive DMFC with XC-72 as anode MPL continuously decays with time, probably due to the fact that the rate of methanol transfer from the reservoir to the anode catalyst layer is lower than that of methanol consumed on the catalyst layer. For the passive DMFC with CNTs as anode MPL, the discharge curves can be divided into three regions. At the early stage, the discharge current decreases within ca. 13 min. Then, the current slightly increases for a period of time. The slight increase in current might be attributed to an increase in cell temperature caused by methanol crossover and to an efficient transport of methanol from the reservoir to the anode catalyst layer, suggesting that the utilization of CNTs within anode MPL is beneficial to the mass transport of methanol. After discharging for ca. 3.5 h, the current starts to continuously decrease as the methanol concentration in the reservoir decreases. For two passive DMFCs, both Faradic efficiency and energy efficiency are calculated. According to previous work [10], Faradic efficiency and energy efficiency for the DMFC with CNTs as anode MPL are calculated to be ca. 71.2% and 21.1%, respectively. However, for the DMFC with XC-72 as anode MPL, Faradic efficiency and energy efficiency are ca. 67.2% and 19.9%, respectively. Clearly, the fuel utilization was improved slightly when using CNTs as anode MPLs, which might be due to an efficient transport of methanol from the reservoir to the anode catalyst layer and to the increased anode reaction rate.

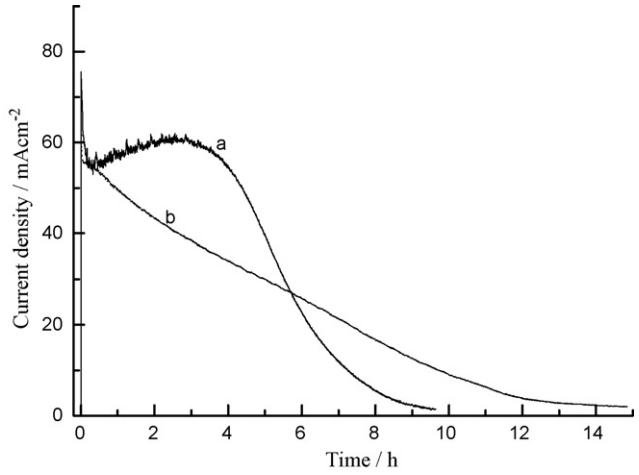

Fig. 2. Transient discharging curves of two passive DMFCs with (a) CNTs and (b) Vulcan XC-72 within the anodic MPLs at a constant voltage of 0.35 V with a start from the cell to be fueled with 6.0 mL of 2 M methanol solution.

3.2. Durability test of a passive DMFC with CNTs as anode MPL material

Since the addition of CNTs into anode MPL of the MEAs significantly improves the performance of the passive DMFCs, thus it is necessary to investigate its durability for long-term operation. Fig. 3 demonstrates a galvanostatic curve of a passive DMFC with CNTs as anodic MPL material at a given current density of 40 mA cm^{-2}. It was found that the discharging voltage keeps at about 0.4 V with some fluctuations. Such fluctuations may be due to the water flooding at cathode side and to the possible change in methanol concentration during the testing. Clearly, the cell voltage only shows very slight decrease with the test time.

3.3. Electrochemical characterizations

To explore the possible reasons for the improved performance of the passive DMFC with CNTs as anode MPL, three anodes with different carbon materials as MPLs were subjected to CV measurements as shown in Fig. 4. By integrating H adsorption/desorption areas, the ESAs of three anodes can be obtained. The ESA of the anode with CNTs as MPL material is calculated to be ca. 32.3 m^2 g$^{-1}_{(Pt)}$, which shows ca. 77.2% higher than that with Vulcan XC-72 with an ESA of ca. 18.2 m^2 g$^{-1}_{(Pt)}$. When using a mixture of CNTs and Vulcan

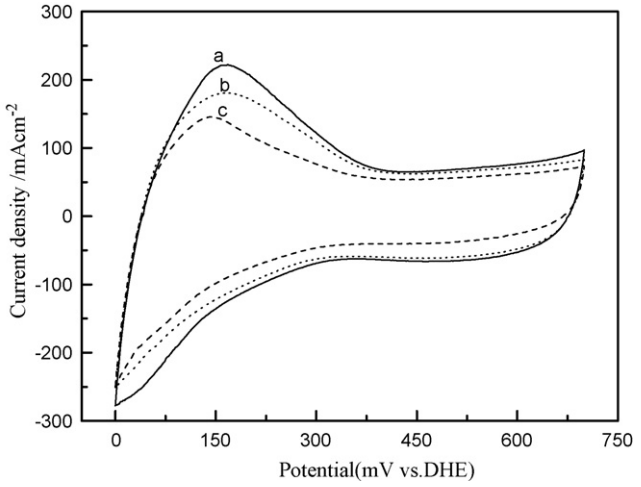

Fig. 4. CVs of anodes with (a) CNTs, (b) a mixture of CNTs and XC-72 carbon and (c) XC-72 carbon as the anode MPL materials at a scan rate of 20 mV s^{-1}.

XC-72 with a mass ratio of 1:1 within the anode MPL, the ESA is ca. 29.5 m^2 $g^{-1}_{(Pt)}$. These results clearly demonstrate that the addition of CNTs into the anode MPL increases the catalyst utilization, thus leading to an improvement in cell performance. The increase in ESA of the anodes with the addition of CNTs might be ascribed to the network formation within the triple-phase regions.

In order to identify the effects of anodic MPL material, EIS of the MEAs in the DMFCs were analyzed. Fig. 5A presents the anode impedance spectra together with fitted curves based on an equivalent circuit model as shown in Fig. 5B. The marked points are the experimental data, while the solid lines are the fitted curves. In this model, the constant phase elements (CPEs) are used to replace ideal capacitors, which are commonly found in conventional equivalent circuit models, to account for the non-uniform structure of the related electrode section. Two CPEs were employed in this particular model in order to account for the influences of anode–membrane interface and the catalyst layer, respectively [18].

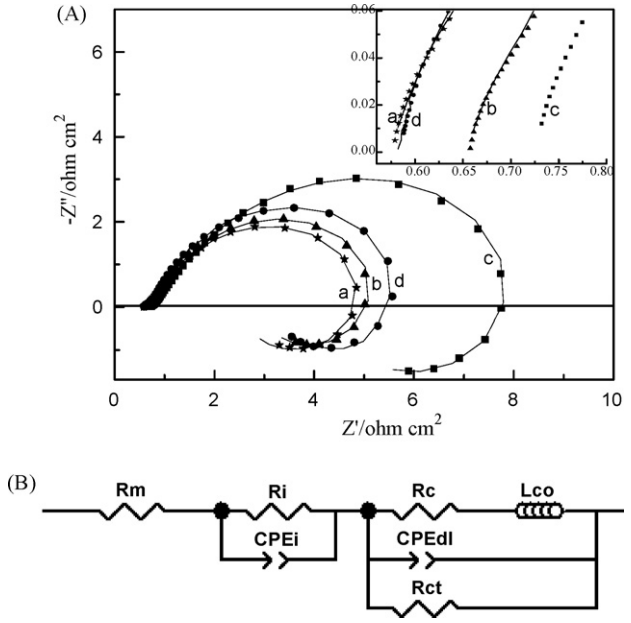

Fig. 5. (A) EIS spectra and (B) equivalent circuit of the DMFCs anodes (vs. DHE) with (a) CNTs (fresh), (b) a mixture of CNTs and XC-72 carbon, (c) XC-72 carbon and (d) CNTs (after long-term operation) within the anode MPLs at a given DC potential of 0.4 V using a 2 M methanol solution.

Thus, the physical meanings of each element employed in the equivalent circuit model (Fig. 5B) are as follows:

(1) R_m denotes the ohmic resistance;
(2) The anode–membrane interface contribution contains CPE_i and R_i, describing the capacitive behavior and contact resistance between the membrane and the catalyst layer, respectively;
(3) The capacitive CPE_{dl} describes the capacitive behavior of the real anode with roughness of the catalyst layer and non-uniform catalyst distribution. The inductance L_{co} means that the current signal follows voltage perturbation with a phase-delay due to slowness of $(CO)_{ad}$ desorption as previously described in Refs. [5,18]. R_c is used to modify the phase-delay and R_{ct} is attributed to the part of the current response which occurs without change in the surface coverage as described previously [5].

The very good agreement between experimental and simulated data shown in Fig. 5A reveals the model validity as shown in Fig. 5B. The fitted parameters are provided in Table 1. As observed, the simulated results of R_i and CPE_i for all the MEAs are nearly the same, which are reasonable because the same anode catalyst and Nafion membrane were used in this work. From the interception with real axis in high-frequency region, the ohmic resistance of a DMFC by using CNTs as anodic MPL materials is slightly smaller than those of the DMFCs with the mixture or Vulcan XC-72 as MPL materials, which could be ascribed to the good electron conduction of CNTs.

Main differences in EIS spectra can be distinguished in the middle-frequency arcs and the loop, which should be attributed to the charge transfer resistances of the anode reaction. The loop might be caused by the adsorbed $(CO)_{ad}$ produced during the methanol electro-oxidation process [5,18]. It can be seen that the anode with CNTs within the MPL shows a smaller arc than that with Vulcan XC-72 at the middle-frequency region and that the values of R_{ct} and L_{co} decrease with the addition of CNTs into the anodic MPL. That is, the charge transfer resistance decreases with the addition of CNTs into the anode MPL increased the EAS of catalyst, which could explain the improved performance of the passive DMFC with CNTs as anodic MPL materials as shown in Figs. 1 and 2.

EIS of the MEA with pure CNTs as anode MPL after long-term operation (more than 350 h) is over-imposed in Fig. 5A (curve d). The fitted parameters are also provided in Table 1. A comparison of curves a and d indicates that only slight changes were observed before and after long-term operation. From Table 1, it can be seen that the ohmic resistance, anode–membrane interface impedance and the $(CO)_{ad}$ desorption impedance increase to some extent after long-term operation, which may be due to the worse contact between catalyst layer and membrane or between catalyst layer and MPL. However, we observed a slight decrease in the charge transfer resistance after long-term operation, which probably suggests that the electrocatalysts were further activated during the discharging process. Small changes in impedance spectra before and after a long-term operation may partly explain good durability of the passive DMFC with CNTs as anodic MPL materials.

Table 1
Fitted parameters for the CPE-based equivalent circuit model for the anode of the passive DMFCs operating at 0.4 V and 25 ± 1 °C.

Parameter	XC-72	CNTs and XC-72	CNTs (fresh)	CNTs (after)
R_m (Ω cm^2)	0.720	0.656	0.576	0.584
R_i (Ω cm^2)	0.100	0.096	0.092	0.155
CPE_i–T (F cm^{-2})	0.284	0.284	0.284	0.108
CPE_i–P	0.625	0.631	0.635	0.732
R_c (Ω cm^2)	5.560	3.208	2.616	3.900
L_{co} (H cm^{-2})	5.955	2.325	1.956	2.388
CPE_{dl}–T (F cm^{-2})	0.259	0.453	0.436	0.323
CPE_{dl}–P	0.740	0.772	0.740	0.812
R_{ct} (Ω cm^2)	10.452	7.376	7.356	7.168

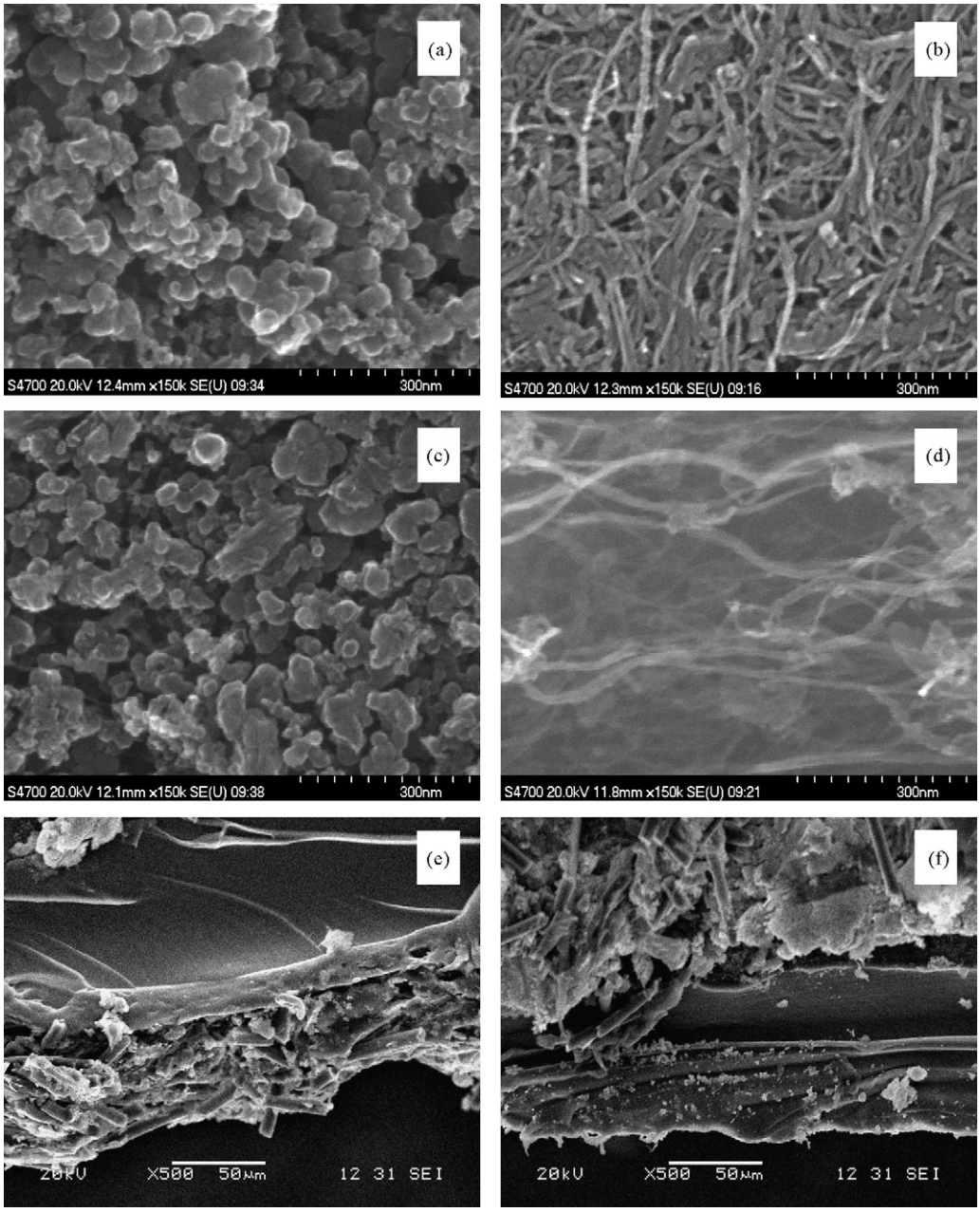

Fig. 6. Top-views of SEM images of the anodic MPLs with XC-72 (a) and CNTs (b); side-views of SEM images of the anodic MPLs with XC-72 (c) and CNTs (d); cross-sectional views of SEM images of the MEA using pure CNTs as anodic MPL materials before (e) and after (f) long-term operation.

3.4. Morphological characteristics of the CNTs in the MPL

Fig. 6 presents the SEM images of the MPLs with CNTs and Vulcan XC-72, respectively. From Fig. 6a, it can be seen that there are some pores distributed within the MPL, which were constituted from the accumulation of XC-72 carbon ball. However, the microstructures of the MPLs with CNTs and Vulcan XC-72 are quite different. For the MPL with CNTs, the uniform and continuous network within the MPL is formed as shown in Fig. 6b. The difference can be distinguished obviously from the side view of SEM images of the MPLs with Vulcan XC-72 and CNTs, as shown in Fig. 6c and d, respectively. It can be seen that there are more pores within the MPL with CNTs than that with Vulcan XC-72, and there was a continuous network within the MPL with CNTs, which would be beneficial to the methanol mass transfer and electron conductivity. It is believed that the network is beneficial for the well-dispersed catalyst ink to merge into the MPL during the fabrication process of the anode, thus decreasing the contact resistance between the catalyst layer and MPL and leading to an increase in electrochemical active surface area, as verified by CV results in Fig. 4.

SEM cross-sectional views of the MEA using pure CNTs as anodic MPL materials before and after long-term operation are shown in Fig. 6e and f, respectively. It can be seen that there is no obvious misalignment of catalyst from membrane and that of MPL from catalyst after long-term operation, indicating that the durability of the passive DMFC with CNTs as anode MPL material is promising for a practical application with an improved performance.

4. Conclusions

In summary, the addition of carbon nanotubes into anodic micro-porous layer of the MEA of the passive DMFCs decreases the

charge transfer resistance of the anode reaction and increases the anode catalyst utilization and improves the methanol mass transfer within the anode, thus leading to a significant improvement in the DMFC performance. The improved performance of the passive DMFC with the addition of CNTs could be due to the network formation within the MPL, which might originate from the one-dimensional structure of CNTs.

Acknowledgements

The work was financially supported by the National '863' High-Tech. Research Programs of China (2006AA05Z136, 2006AA04Z342, 2007AA05Z141, 2008AA05Z102), the National Natural Science Foundation of China (20706056) and the 100 People Plan Program of the Chinese Academy of Sciences.

References

[1] Y.H. Chan, T.S. Zhao, R. Chen, C. Xu, J. Power Sources 178 (2008) 118–124.
[2] Z. Guo, A. Faghri, Int. Commun. Heat Mass Trans. 35 (2008) 225–239.
[3] D. Kim, E.A. Cho, S.A. Hong, I.H. Oh, H.Y. Ha, J. Power Sources 130 (2004) 172–177.
[4] S.K. Kamarudin, W.R.W. Daud, S.L. Ho, U.A. Hasran, J. Power Sources 163 (2007) 743–754.
[5] T.V. Reshetenko, H.T. Kim, H.J. Kweon, Electrochim. Acta 53 (2008) 3043–3049.
[6] M.S. Yazici, J. Power Sources 166 (2007) 424–429.
[7] C. Lin, T. Wang, F. Ye, Y. Fang, X. Wang, Electrochem. Commun. 10 (2008) 255–258.
[8] R. Chen, T.S. Zhao, Electrochem. Commun. 9 (2007) 718–724.
[9] G. Wang, G. Sun, Q. Wang, S. Wang, J. Cui, Y. Gao, Q. Xin, J. Power Sources 180 (2008) 176–180.
[10] J.G. Liu, T.S. Zhao, R. Chen, C.W. Wong, Electrochem. Commun. 7 (2005) 288–294.
[11] Y.M. Kim, K.W. Park, J.H. Choi, I.S. Park, Y.E. Sung, Electrochem. Commun. 5 (2003) 571–574.
[12] W.C. Choi, J.D. Kim, S.I. Woo, J. Power Sources 96 (2001) 411–414.
[13] H.L. Lin, T.L. Yu, L.N. Huang, L.C. Chen, K.S. Shen, G.B. Jung, J. Power Sources 150 (2005) 11–19.
[14] Z. Wei, S. Wang, B. Yi, J. Liu, L. Chen, W. Zhou, W. Li, Q. Xin, J. Power Sources 106 (2002) 364–369.
[15] G. Girishkumar, T.D. Hall, K. Vinodgopal, P.V. Kamat, J. Phys. Chem. B 110 (2006) 107–114.
[16] G. Wu, B.Q. Xu, J. Power Sources 174 (2007) 148–158.
[17] M. Carmo, V.A. Paganin, J.M. Rosolen, E.R. Gonzalez, J. Power Sources 142 (2005) 169–176.
[18] N.Y. Hsu, S.C. Yen, K.T. Jeng, C.C. Chien, J. Power Sources 161 (2006) 232–239.
[19] K.T. Jeng, C.C. Chien, N.Y. Hsu, W.M. Huang, S.D. Chiou, S.H. Lin, J. Power Sources 164 (2007) 33–41.
[20] S.K. Wang, F.G. Tseng, T.K. Yeh, C.C. Chieng, J. Power Sources 167 (2007) 413–419.
[21] K.T. Jeng, C.C. Chien, N.Y. Hsub, S.C. Yen, S.D. Chiou, S.H. Lin, W.M. Huang, J. Power Sources 160 (2006) 97–104.
[22] M.C. Tsai, T.K. Yeh, C.Y. Chen, C.H. Tsai, Electrochem. Commun. 9 (2007) 2299–2303.
[23] C.H. Wang, H.Y. Du, Y.T. Tsai, C.P. Chen, C.J. Huang, L.C. Chen, K.H. Chen, H.C. Shih, J. Power Sources 171 (2007) 55–62.
[24] P. Wu, B. Li, H. Du, L. Gan, F. Kang, Y. Zeng, J. Power Sources 192 (2009) 324–329.
[25] M.A. Abdelkareem, N. Nakagawa, J. Power Sources 162 (2006) 114–123.
[26] J.G. Liu, G.Q. Sun, F.L. Zhao, G.X. Wang, G. Zhao, L. Chen, B.L. Yi, Q. Xin, J. Power Sources 133 (2004) 175–180.
[27] J.G. Liu, T.S. Zhao, Z.X. Liang, R. Chen, J. Power Sources 153 (2006) 61–67.